# Small-strain shear modulus of silty sands: the role of sample preparation method

YUTANG CHEN\* and JUN YANG†

Establishing the influence of sample preparation method on shear wave velocity or associated small-strain shear modulus  $(G_0)$  of silty sands is a subject of considerable interest. This paper presents an attempt to address this topic through a comprehensive experimental programme covering four sample preparation methods. The experiments were conducted on clean Toyoura sand and its mixtures with two types of fines of different sizes. For each sample preparation method, a range of void ratio and confining stress was investigated to obtain a comprehensive view of the influence of sample preparation and its interplay with other factors. One of the notable findings is that, compared with clean sand, the difference of  $G_0$  induced by different sample reconstitution methods can be much enlarged for silty sand, and the influence is coupled with the size disparity ratio of the mixtures. The reduction of  $G_0$  due to the presence of fines also depends on sample preparation method and for smaller fines the reduction is more significant. A careful examination of the X-ray images of the specimens made by different methods suggests that the observed effects are mainly associated with the different contact conditions of coarse and fine grains.

KEYWORDS: granular materials; microstructure; modulus of elasticity; sample preparation; shear modulus; shear wave velocity; silty sands; soil fabric

# INTRODUCTION

The shear wave velocity ( $V_s$ ) or its associated small-strain shear modulus ( $G_0$ ) of granular soils has been a subject of long-standing interest in geotechnical engineering (Hardin & Richart, 1963; Stokoe *et al.*, 1999; Clayton, 2011). Extensive use of  $V_s$  and  $G_0$  can be found in many major engineering applications, ranging from earthquake ground response, foundation vibration and liquefaction evaluation to performance-based design of underground structures. Numerous studies have been conducted to characterise  $V_s$  and  $G_0$  for sands, and it is now widely acknowledged that the  $G_0$  of sand is highly influenced by void ratio and effective confining stress. However, even under the same void ratio and confining stress, the use of different sample reconstitution methods (e.g. dry deposition and moist tamping) may lead to some differences in measured  $V_s$  or  $G_0$  (Gu *et al.*, 2015; Shi *et al.*, 2021).

Often, natural sand is not clean, but contains a certain quantity of fines. A number of studies have been conducted to investigate the influence of fines content on the  $G_0$  of silty sands (Iwasaki & Tatsuoka, 1977; Salgado *et al.*, 2000; Chien & Oh, 2002; Sahaphol & Miura, 2005; Rahman *et al.*, 2012; Choo & Burns, 2014; Wichtmann *et al.*, 2015; Goudarzy *et al.*, 2016; Yang & Liu, 2016; Payan *et al.*, 2017; Liu & Yang, 2018; Shi *et al.*, 2020). These studies showed that the presence of fines will alter  $G_0$  values of clean sand but the measured variations appear to be diverse. To account for the influence of fines, several studies have used the equivalent skeleton void ratio (Thevanayagam *et al.*, 2002;

Rahman *et al.*, 2008; Goudarzy *et al.*, 2016) as the state variable for silty sands. However, the use of the skeleton void ratio may result in underestimation of shear stiffness at high fines content or when the size ratio between coarse and fine particles is low (Wichtmann *et al.*, 2015; Liu & Yang, 2018). The key idea of the equivalent skeleton void ratio is to use a parameter, often denoted as b, to quantify the fraction of fines participating in the force transfer. Among recent notable attempts to account for the influence of fines is that by Yang & Liu (2016), who showed that  $G_0$  values for both clean sand and sand–fines mixtures can be unified through the state parameter defined in the critical state theory.

In a similar way to when using clean sand, various sample reconstitution methods have been adopted to prepare silty sand specimens in the literature, as shown in Table 1. It is hypothesised that the sample preparation method may contribute to the reported diverse effects of fines on  $G_0$ , since the small particles in silty sand specimens may alter the packing pattern when the specimens are remoulded by different methods. However, no experimental data are available in the current literature for examining this hypothesis. Existing studies on sample preparation methods have focused mainly on large-strain undrained shear behaviour (Wood et al., 2008; Yamamuro et al., 2008; Yang et al., 2008; Sze & Yang, 2014; Zhu et al., 2021). In this paper, an attempt is made to explore the role of the sample preparation method in altering the small-strain shear modulus for both clean and silty sands. To obtain a comprehensive view of the effect of sample preparation method and the possible interplay with other factors, the experimental programme covered four commonly used reconstitution methods and, for each method, a range of states in terms of post-consolidation void ratio and confining stress was investigated. The X-ray tomography technique was utilised to study the microstructure or fabric of the specimens produced using different methods. This paper presents the first-hand data along with interpretation and analysis. A microscopic mechanism is also proposed to explain the observed variations of  $G_0$  values associated with different sample preparation methods.

Manuscript received 7 February 2023; revised manuscript accepted 4 September 2023. First published online ahead of print 3 November 2023

Discussion on this paper closes on 1 August 2024, for further details see p. ii.

\* Department of Civil Engineering, The University of Hong Kong, Pokfulam, Hong Kong, China.

† Department of Civil Engineering, The University of Hong Kong, Pokfulam, Hong Kong, China (Orcid:0000-0002-0250-5809).

Table 1. Literature studies on  $G_0$  of silty sands

References	Base sand	Maximum FC	SPM	Dry or saturated
Iwasaki & Tatsuoka (1977)	Iruma sand	14	AP	D&S
Salgado et al. (2000)	Ottawa sand	20	SP	S
Chien & Oh (2002)	Yunlin hydraulic sand	30	MT	S
Sahaphol & Miura (2005)	Volcanic soil	100	AP	S
Choo & Burns (2014)	ASTM sand	100	DD	D
Choo & Burns (2015)	ASTM sand	100	DD	D
Wichtmann et al. (2015)	Dorsten natural quartz sand	20	AP	D
Yang & Liu (2016)	Toyoura sand	30	MT	S
Goudarzy et al. (2016)	Houston sand	40	DD	D
Payan et al. (2017)	White sand and blue sand	100	DT	D
Liu & Yang (2018)	Toyoura sand and Fujian sand	10	MT	S
Shi et al. (2020)	Calcareous sand	100	DT	S

Note: SPM, sample preparation method; MT, moist tamping; AP, air pluviation; SP, slurry deposition; DD, dry deposition; DT, dry tamping; D, dry; S, saturated.

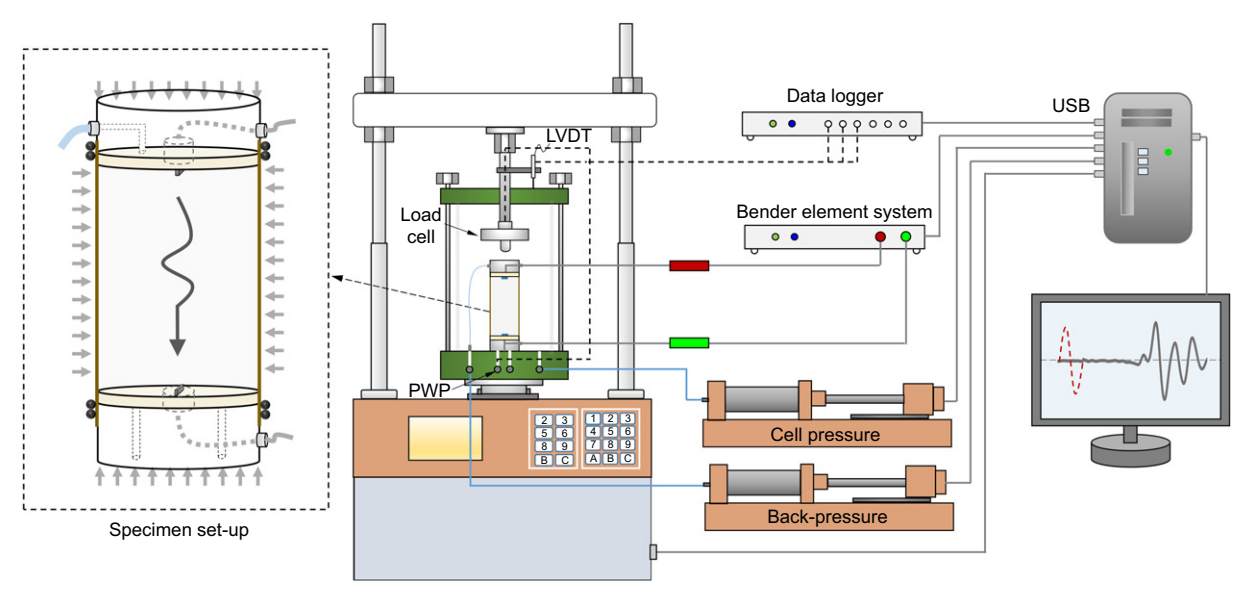


Fig. 1. Schematic diagram of the triaxial apparatus used in this study

# TESTING MATERIAL AND TESTING PROGRAMME *Testing apparatus*

Shear wave measurement was performed by a pair of bender elements embedded in a triaxial apparatus as shown in Fig. 1. The specimen size is 50 mm dia. and 100 mm high, and the effective confining stress is controlled by the cell pressure and back-pressure controllers. The shear waves propagate in the vertical direction and polarise in the horizontal direction, capturing the small-strain shear modulus in the vertical plane. Careful calibration of bender element functions was conducted to determine the system delay, including the response time of the bender elements and the travel time in the cables. The maximum shear modulus  $G_0$  is calculated based on equation (1)

$$G_0 = \rho V_s^2 \tag{1}$$

where  $\rho$  is the mass density involved in the wave propagation and  $V_s$  is the shear wave velocity. Gu *et al.* (2015) and Youn *et al.* (2008) discussed the dispersion of shear waves in saturated soils and suggested to use the effective mass density to convert  $V_s$  to  $G_0$  for soils with high permeability. Since all the clean and silty specimens in this study were tested under saturated conditions, the mass densities were corrected according to the method described by Gu *et al.* (2015). In

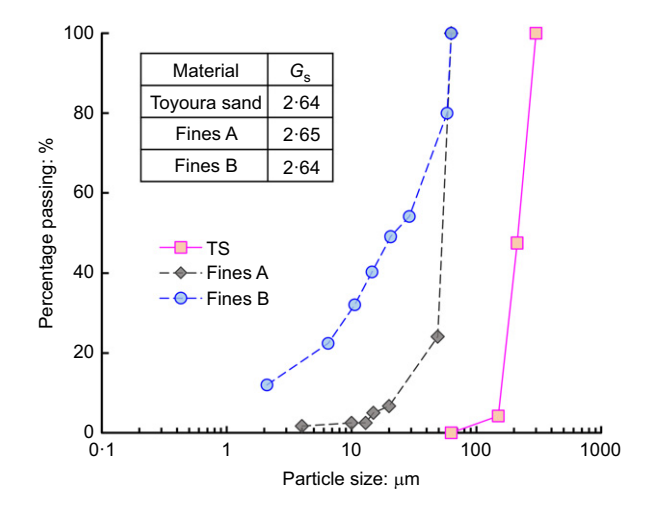


Fig. 2. Particle size distribution curves of the test materials

each bender element test, a set of sinusoid signals at various frequencies (from 2 to 40 kHz) was used as the excitation, and the received signals were examined in a whole view to better identify the arrival time of shear wave. It was found

that signals at the input frequency of 10 kHz allowed the first arrival of shear waves to be identified consistently and reliably, which is in agreement with the observations of previous studies (Yang & Gu, 2013; Gu et al., 2015; Yang & Liu, 2016). Among various methods that are used to determine the travel time of elastic waves (e.g. Yamashita et al., 2009; Alvarado & Coop, 2012; Yang & Gu, 2013; Gu et al., 2015), the first arrival method in the time domain, when applied properly, has shown to be a reliable and simple method for both clean sand and sand with fines.

#### Materials and specimen preparation

The clean Toyoura sand was chosen as the base sand and two crushed silica fines of different sizes were adopted as the additives. Artificially created mixtures enable good control of grain characteristics and facilitate experimental repeatability such that any more complex effects or uncertainties are removed. Fig. 2 shows the particle size distribution curves along with the physical properties of the materials. Toyoura sand is a uniform quartz sand with sub-angular to subrounded grains, whereas the crushed silica fines A and B are composed of non-plastic angular grains, with fines B having a smaller mean grain size. In the following discussion, shorthand notations are used for the clean and mixed sands; for example, TS stands for clean Toyoura sand; TSSA10 and

TSSB10 denote Toyoura sand mixed with fines A of 10% by mass and fines B of 10% by mass, respectively. Four methods commonly used to reconstitute specimens in soil mechanics laboratory were investigated in this study. These methods are illustrated in Fig. 3 and are briefly described below.

(a) Moist tamping (MT): MT has been widely employed in the laboratory investigation of liquefaction problems because it is able to create very loose specimens with capillary force (Ishihara, 1993; Yang & Wei, 2012; Zhu et al., 2021). By adjusting tamping energy, the specimen can also be made in a relatively dense state. Each specimen was prepared in five layers at the layer thickness of  $\sim$ 20 mm. For a desired void ratio, an amount of moist sand at 5% water content was measured and slowly deposited into the split mould. The soil layer was then carefully levelled with a brush and compacted to the desired height with a bronze tamper (47.46 mm dia.). The surface was carefully scraped to enhance the connection between the two neighbouring layers before the construction of the next layer. Owing to the capillary force in the moist sand, sand grains can hold together and therefore relatively higher compaction energy is needed to achieve the dense state in the MT method. Such a loading history may affect the contact number and the uniformity of the

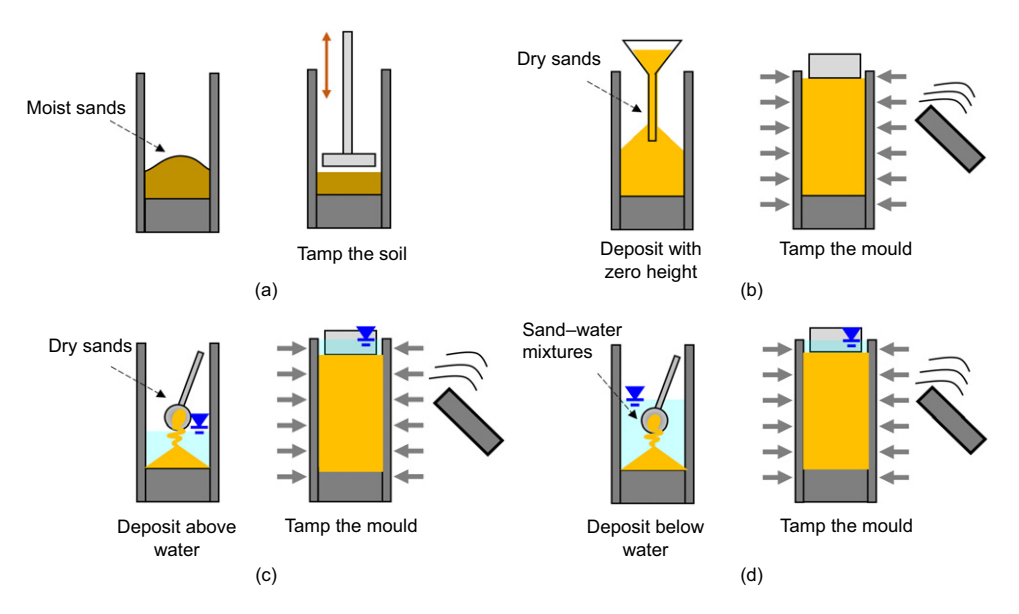


Fig. 3. Schematic illustration of sample preparation methods in this study: (a) MT; (b) DD; (c) WSA; (d) WSB. A full-colour version of this figure can be found on the ICE Virtual Library (www.icevirtuallibrary.com)

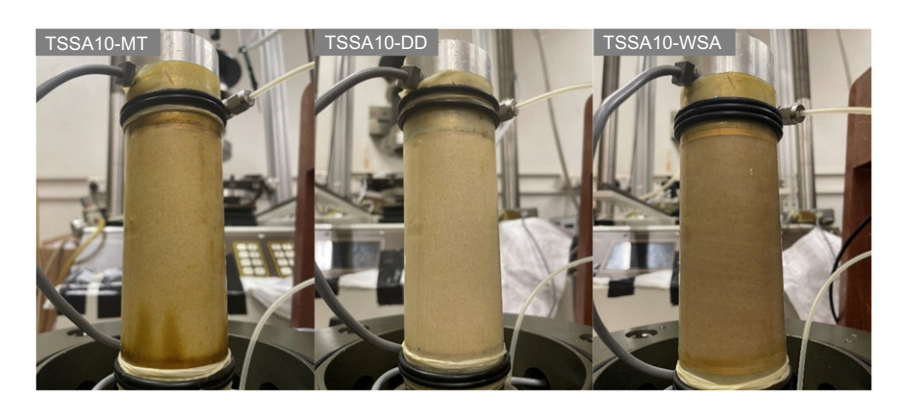


Fig. 4. Photographs of specimens produced by different reconstitution methods

Table 2. Summary of testing series

Material – SPMs	State 1 $(e, \sigma')$	State 2 $(e, \sigma')$	State 3 $(e, \sigma')$	State 4 $(e, \sigma')$
TS-MT	(0.799, 50)	(0.796, 100)	(0.790, 200)	(0.784, 400)
	(0.794, 50)	(0.790, 100)	(0.785, 200)	(0.779, 400)
	(0.871, 50)	(0.867, 100)	(0.862, 200)	(0.855, 400)
	(0.755, 50)	(0.752, 100)	(0.748, 200)	(0.743, 400)
	(0.874, 50)	(0.870, 100)	(0.864, 200)	(0.857, 400)
	(0.759, 50)	(0.756, 100)	(0.752, 200)	(0.747, 400)
TS-DD	(0.791, 50)	(0.787, 100)	(0.783, 200)	(0.776, 400)
	(0.858, 50)	(0.851, 100)	(0.844, 200)	(0.835, 400)
	(0.796, 50)	(0.792, 100)	(0.786, 200)	(0.780, 400)
	(0.734, 50)	(0.731, 100)	(0.726, 200)	(0.721, 400)
	(0.790, 50)	(0.786, 100)	(0.780, 200)	(0.773, 400)
	(0.862, 50)	(0.855, 100)	(0.847, 200)	(0.837, 400)
	(0.746, 50)	(0.743, 100)	(0.738, 200)	(0.733, 400)
TS-WSA	(0.789, 50)	(0.785, 100)	(0.779, 200)	(0.773, 400)
	(0.723, 50)	(0.720, 100)	(0.716, 200)	(0.711, 400)
	(0.791, 50)	(0.787, 100)	(0.781, 200)	(0.774, 400)
TS-WSB	(0.795, 50)	(0.791, 100)	(0.786, 200)	(0.779, 400)
	(0.724, 50)	(0.721, 100)	(0.717, 200)	(0.711, 400)
	(0.811, 50)	(0.807, 100)	(0.802, 200)	(0.795, 400)
	(0.754, 50)	(0.750, 100)	(0.745, 200)	(0.739, 400)
	(0.706, 50)	(0.703, 100)	(0.699, 200)	(0.693, 400)
TSSA10-MT	(0.789, 50)	(0.785, 100)	(0.779, 200)	(0.773, 400)
155/110 1411	(0.752, 50)	(0.748, 100)	(0.744, 200)	(0.739, 400)
	(0.872, 50)	(0.867, 100)	(0.860, 200)	(0.850, 400)
TSSA10-DD	(0.780, 50)	(0.775, 100)	(0.768, 200)	(0.760, 400)
155/110 DD	(0.746, 50)	(0.742, 100)	(0.736, 200)	(0.729, 400)
	(0.838, 50)	(0.830, 100)	(0.819, 200)	(0.806, 400)
	(0.790, 50)	(0.783, 100)	(0.775, 200)	(0.765, 400)
TSSA10-WSA	(0.709, 50)	(0.706, 100)	(0.701, 200)	(0.695, 400)
155/110-W5/1	(0.756, 50)	(0.752, 100)	(0.746, 200)	(0.739, 400)
	(0.701, 50)	(0.697, 100)	(0.692, 200)	(0.686, 400)
	(0.777, 50)	(0.772, 100)	(0.765, 200)	(0.757, 400)
TSSA10-WSB	(0.688, 50)	(0.685, 100)	(0.681, 200)	(0.675, 400)
133A1U-W3D	(0.787, 50)	(0.683, 100) (0.782, 100)	(0.681, 200) (0.775, 200)	(0.767, 400)
TSSB10-MT	(0.787, 50) (0.798, 50)	(0.782, 100) (0.794, 100)	(0.773, 200) (0.789, 200)	
1 22D10-M1	\ / /		` ' '	(0.782, 400)
TSSB10-DD	(0.687, 50)	(0.684, 100)	(0.681, 200)	(0.676, 400)
133010-DD	(0.788, 50)	(0.780, 100)	(0.771, 200)	(0.759, 400)
	(0.677, 50)	(0.673, 100)	(0.668, 200)	(0.661, 400)

Note: SPM, sample preparation method; e, void ratio;  $\sigma'$ , effective confining stress (kPa).

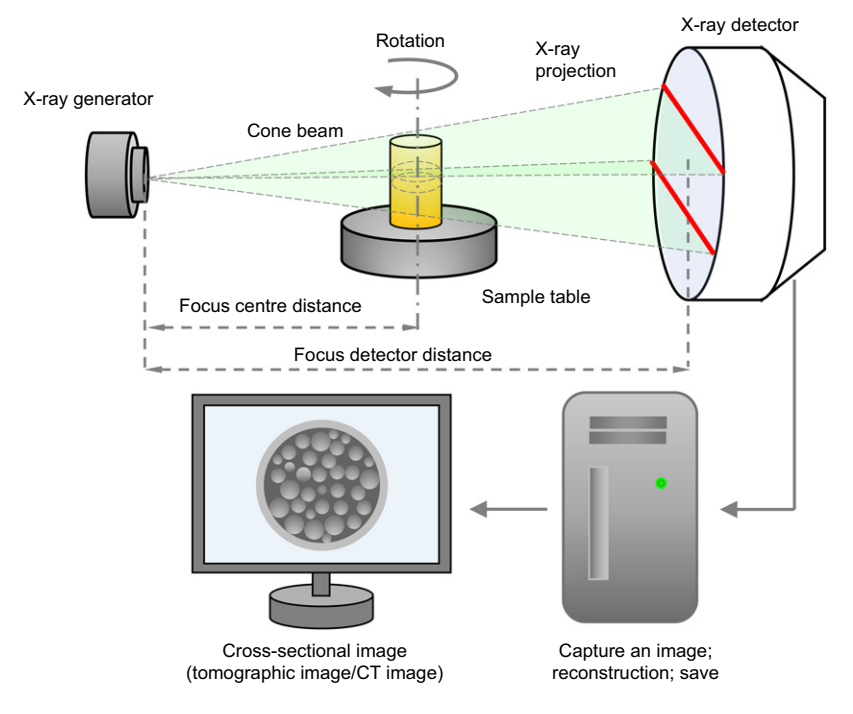


Fig. 5. Schematic illustration of the working principle of micro CT

- contact forces, thus resulting in an increased stiffness (Gu et al., 2015), and this constitutes part of the effect of sample preparation. For sand–fines mixtures, the technique has a better performance in preventing segregation than other sample preparation methods.
- (b) Dry deposition (DD): DD is another common technique to prepare sand specimens with the advantage of convenience (Lade & Yamamuro, 1997; Sze & Yang, 2014). In this study, oven-dried sand at a predetermined mass was deposited through a funnel into a split mould. The funnel tip was maintained at a zero height of drop above the surface of the sand deposit to give the lowest possible density. Tapping was then conducted uniformly around the periphery of the mould using a rubber

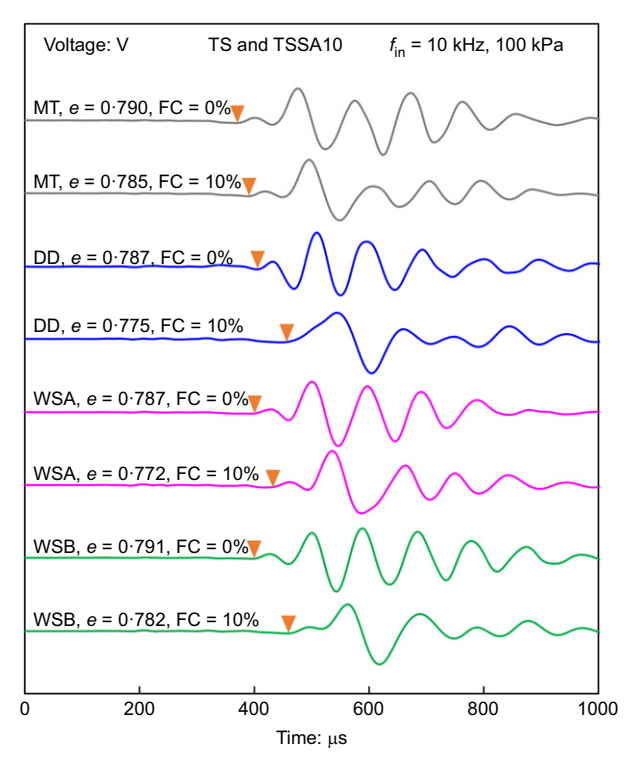


Fig. 6. Shear wave signals in saturated TS and TSSA10 specimens made by different methods

- hammer to achieve the target density. Note that the DD method is somewhat different from the method known as air pluviation or sand raining (Mulilis et al., 1977; Wichtmann et al., 2020) in that the latter method involves pouring dry sand in the air from a nozzle or a sieve at a certain rather than zero height into a mould. Nevertheless, both methods share similar principles that are distinctly different from that of MT. For sand-fines mixtures, great care was taken to minimise possible segregation. To check the quality of the DD specimens, fines contents in several TSSB10 specimens were measured. The average fines content in the top layer is 10.83% while the fines content in the bottom layer is 9.06% on average, confirming that no segregation occurred. The photograph of a representative DD specimen is given in Fig. 4.
- (c) Water sedimentation above (WSA) and below water (WSB): water sedimentation is thought to be the method that can better simulate the in situ soil fabric. In the literature, experimental data on shear wave velocity in sand specimens made by water sedimentation are rather limited. For WSA, dry sand was deposited into the de-aired water spoon by spoon. The dry sand in each spoon was measured 7–8 g, and the spoon was placed close to the water surface. For WSB, dry sand was mixed with de-aired water first and then deposited below the water surface spoon by spoon. The mixture of water and sand in each spoon was measured 11-12 g. After depositing the sand, very light tapping was conducted to achieve a denser state (Fig. 3). Unlike the DD method, the tapping needs to be very light, otherwise the specimen may liquefy, especially when preparing specimens of sand-fines mixtures. Since deposition was conducted spoon by spoon and given low fines content, segregation is considered insignificant. Note that the range of void ratio that can be achieved by water sedimentation is limited compared with the MT method, and it is difficult to produce loose specimens using this method.

For MT and DD specimens, they were flushed with carbon dioxide and de-aired water for a given time to achieve better saturation. For WSA and WSB specimens, although they were already deposited in de-aired water, another round of de-aired water flushing was conducted to reduce possible air

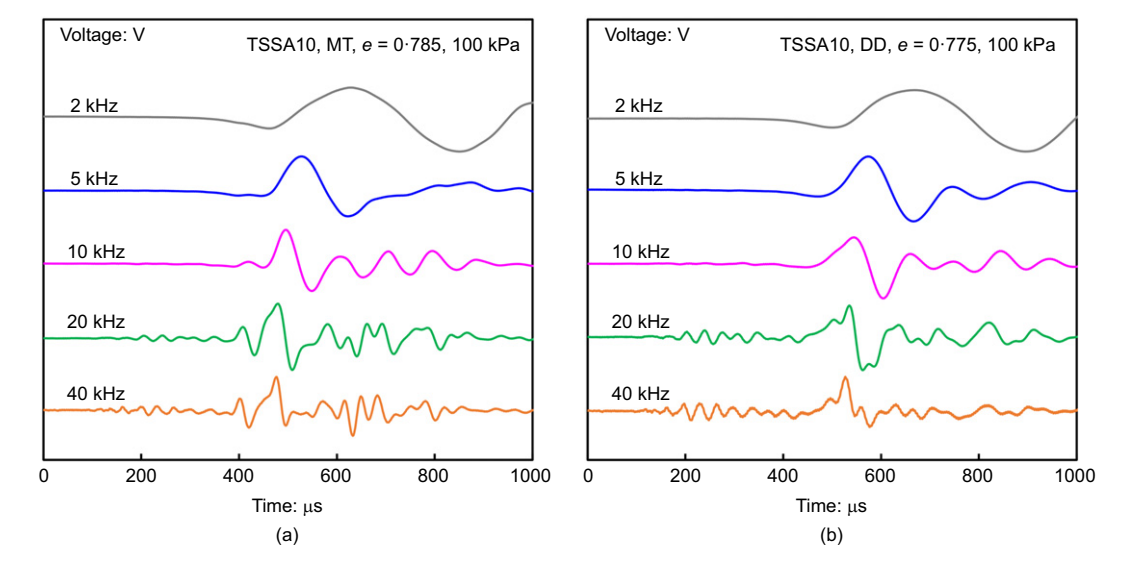


Fig. 7. Shear wave signals excited by different frequencies in saturated TSSA10 specimens made by MT and DD methods: (a) MT method; (b) DD method

bubbles tracked in the specimens. Full saturation for all specimens was further ensured by applying back-pressure, with the Skempton *B*-value larger than 0.95. After the saturation process, each specimen was subjected to isotropic confining stress in stages, typically at 50, 100, 200 and 400 kPa.

In this study, the MT, DD, WSA and WSB methods were used to produce TS and TSSA10 specimens at a wide range of void ratios, to investigate systematically the influence of sample reconstitution method on the shear modulus of clean and silty sand. For TSSB10 specimens, MT and DD methods were used to explore whether the fines type would influence the observations obtained from the test series on TSSA10

specimens. A higher fines content was not considered in the present study because the attention is currently focused on the influence of low fines content. A summary of the test series is given in Table 2.

#### Microscale investigation

A micro CT was used to detect the internal structures of clean and silty sand specimens. As shown in Fig. 5, the system contains three principal components, including a high-power X-ray generator, a rotary sample table and an X-ray detector. The generator can emit highly penetrating X-rays after the warm-up process. When passing through the

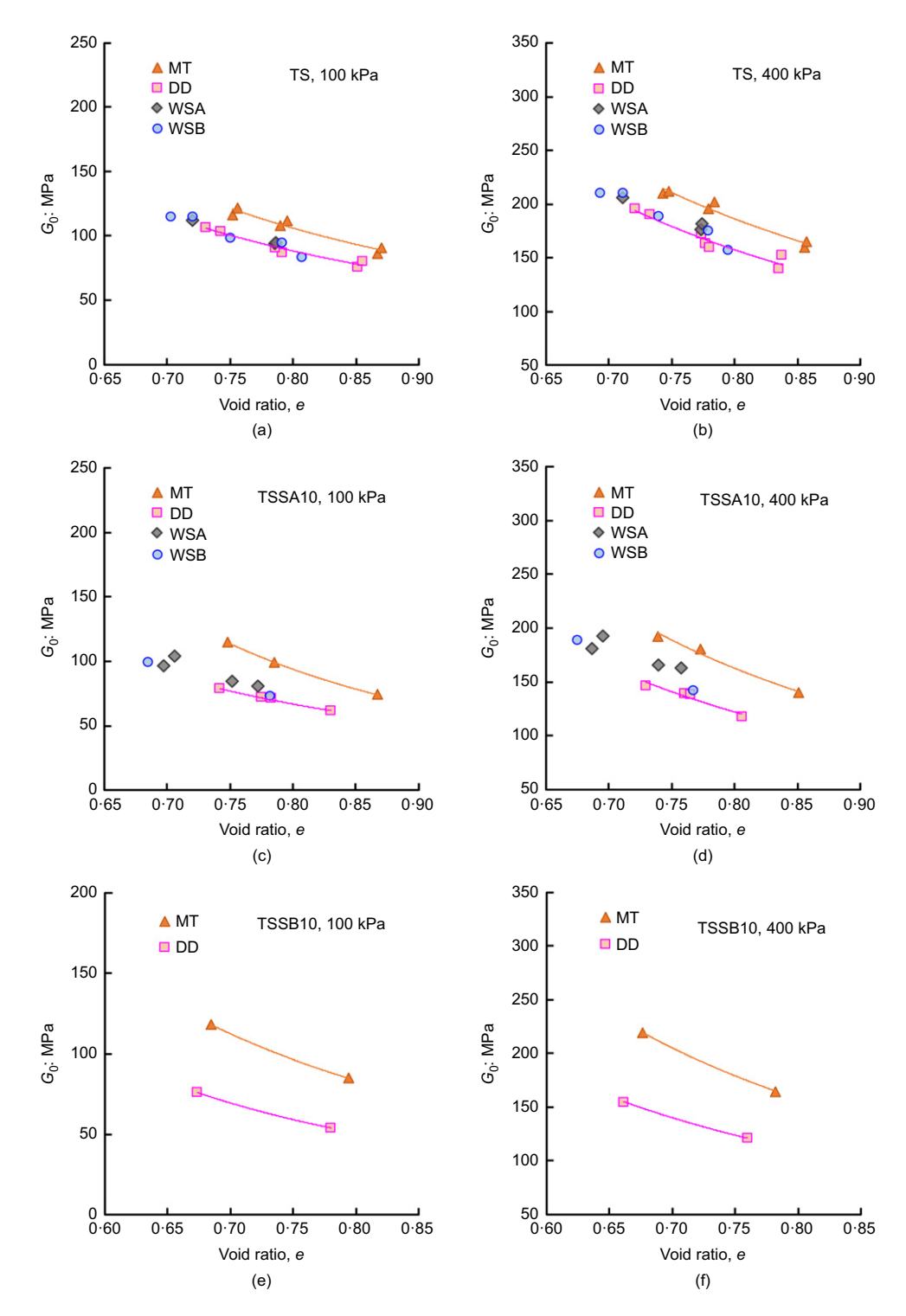


Fig. 8. Variation of shear modulus with void ratio affected by sample preparation method: (a), (b) TS; (c), (d) TSSA10; (e), (f) TSSB10

targeted object, the X-ray can be attenuated due to absorption or reflection by the object. The remaining X-rays reach the detector and the projection information is recorded. The detected object needs to rotate 360° with the sample table at a very small angle and the detector records all the received information at each angle. After scanning, a highperformance computer is required for image reconstruction based on the projections to obtain the cross-sectional image. The CT scanning mode used in this study is the cone-beam mode which can obtain images of horizontal sections at different heights of the specimen, and the vertical distance between two consecutive sections is as small as 8 µm. To better identify large and small particles, the Toyoura sand was sieved and only the particles between 212 and 300  $\mu m$ were used. The scanned samples were prepared by moist tamping and dry deposition methods in an acrylic mould. The sample size was 21.55 mm dia. and 20 mm high, and the void ratio was prepared at  $\sim 0.750$ .

#### TEST RESULTS AND ANALYSIS

Effects of sample preparation and fines on shear wave signals Figure 6 shows received shear wave signals excited at 10 kHz for TS and TSSA10 specimens under the confining stress of 100 kPa. All signals in TS specimens display a small peak before the succeeding large peak, which is consistent with the observations by Yang & Gu (2013) and Gu et al. (2015) on specimens of uniform glass beads and clean Toyoura sand. The first arrival of a shear wave can be

clearly identified, as marked by a downward triangle in each waveform. For consistency, signals at the input frequency of 10 kHz were used to determine the shear wave velocity and shear modulus in this study. For TSSA10 specimens, the shear wave signals of MT, WSB and WSA specimens are quite similar to those of clean sand specimens, and this is consistent with the observation of Yang & Liu (2016). However, the signal in the TSSA10 specimen formed by the DD method is obviously different from others in that the small peak is gone. A similar observation was also made in signals generated at frequencies of 5 kHz and 20 kHz, as shown in Fig. 7, in which the signals excited at different frequencies in TSSA10 specimens made by MT and DD methods are given. This interesting observation has never been reported before; it is likely to be related to the microstructure of TSS specimens formed by the DD method, as will be shown later. Overall, the presence of fines is found to increase the shear wave travel time and thus to decrease the shear stiffness regardless of sample preparation methods.

Effect of sample preparation on  $G_0$  in clean and silty sands A more comprehensive view of  $G_0$  values of TS, TSSA10 and TSSB10 specimens measured under various conditions is displayed in Fig. 8, where  $G_0$  values are shown as a function of the void ratio for specimens for the confining stress of 100 and 400 kPa. Evidently,  $G_0$  is dependent on void ratio, confining stress and sample preparation method. Under

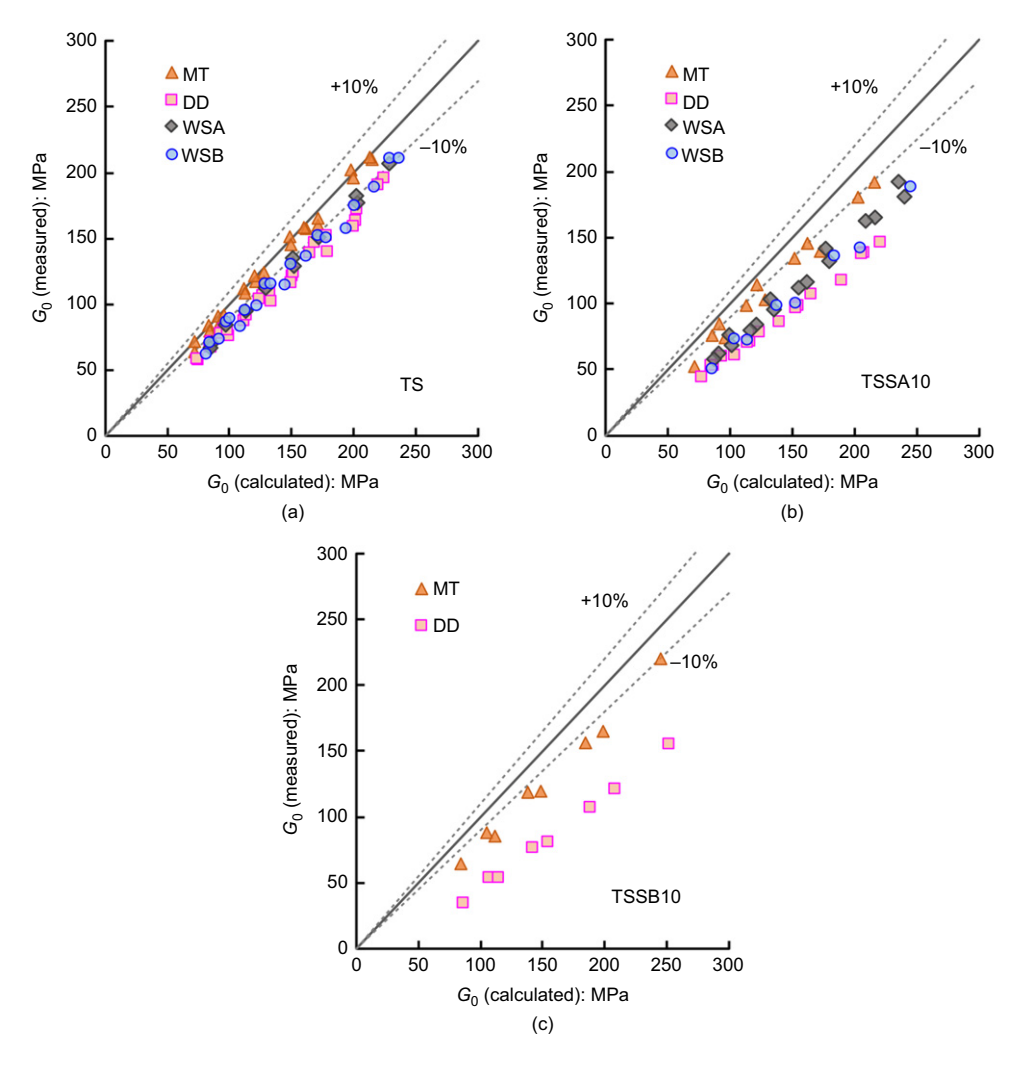


Fig. 9. Comparison of measured and calculated  $G_0$  values: (a) TS; (b) TSSA10; (c) TSSB10

otherwise similar conditions,  $G_0$  increases with increasing confining stress and with decreasing void ratio. As for the effect of sample preparation method, it appears to be complicated. For TS and TSSA10, the measured  $G_0$  values of MT specimens are notably higher compared with those of DD, WSA and WSB specimens. The differences in measured  $G_0$  values of DD, WSA and WSB specimens are, however, insignificant for TS, but tend to become visible for TSSA10, with the DD specimens showing the lowest  $G_0$  values. A notable feature of the results of TSSB10 is that the difference between  $G_0$  values of MT and DD specimens becomes much

more significant compared with that for TSSA10, suggesting the interplay between sample preparation and fines inclusion.

Based on bender element tests on Toyoura sand specimens prepared by moist tamping, Gu et al. (2015) determined the two parameters in Hardin's formula for  $G_0$ . An attempt is made here to estimate  $G_0$  using this formula and the determined parameters. Fig. 9 shows measured  $G_0$  values plotted against calculated ones for TS, TSSA10 and TSSB10. It is clear that for TS specimens made by MT, the measurements are in good agreement with the calculated ones, whereas the measurements for TS specimens made by

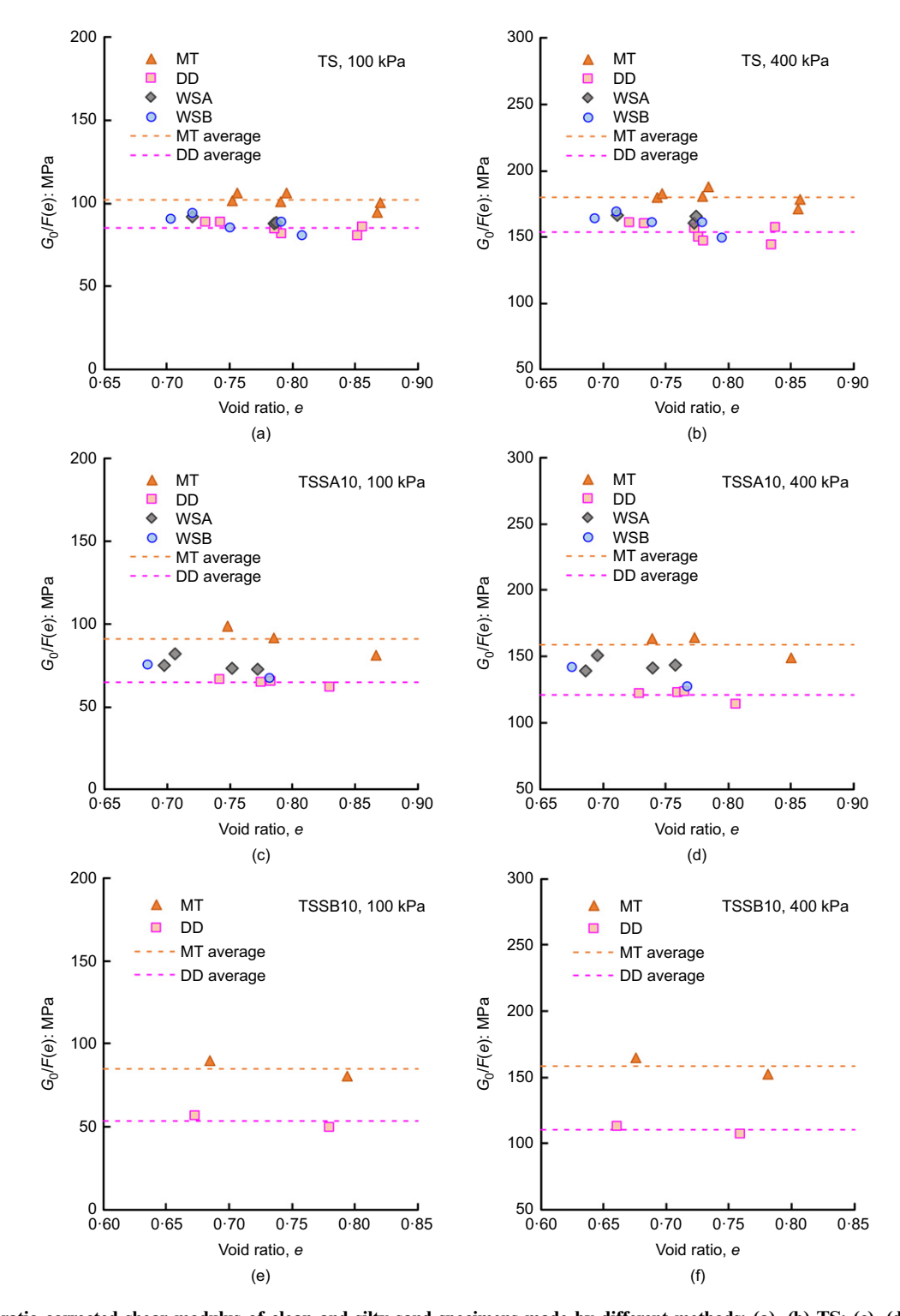


Fig. 10. Void ratio-corrected shear modulus of clean and silty sand specimens made by different methods: (a), (b) TS; (c), (d) TSSA10; (e), (f) TSSB10. A full-colour version of this figure can be found on the ICE Virtual Library (www.icevirtuallibrary.com)

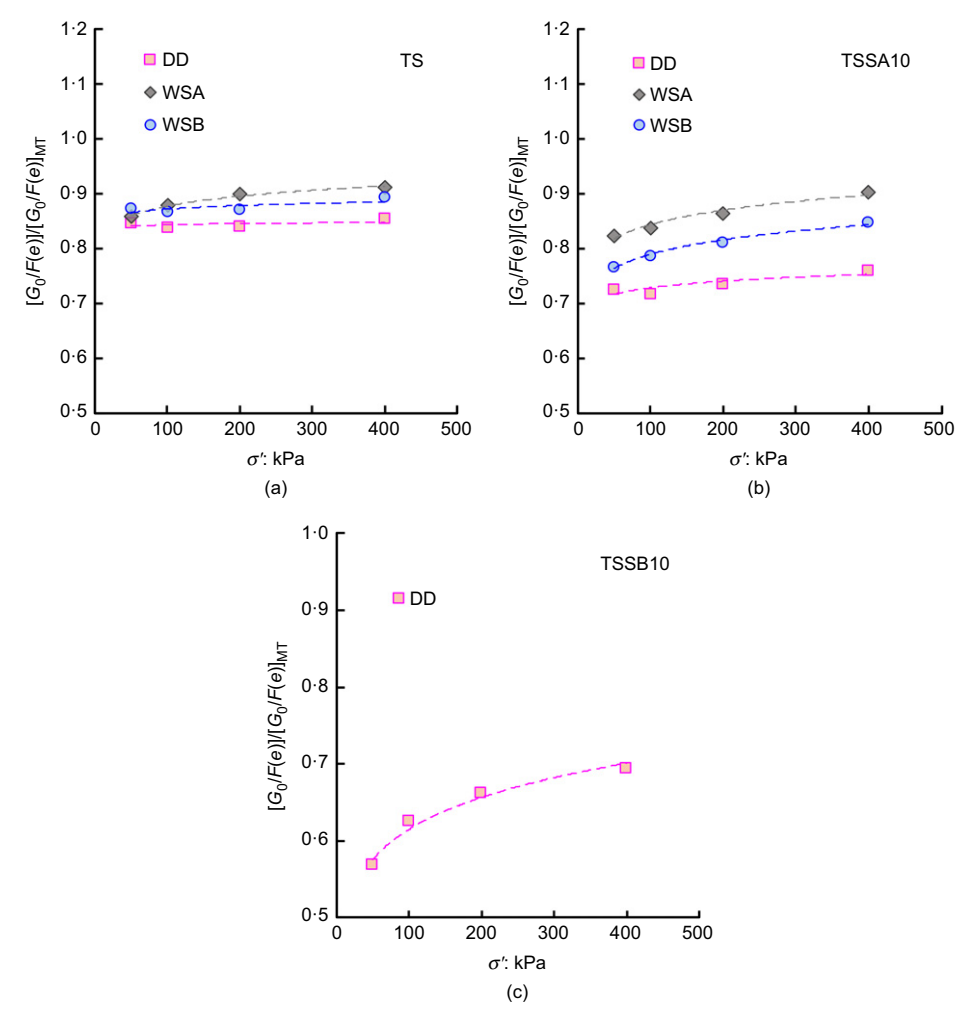


Fig. 11. Differences in shear modulus induced by different sample preparation methods: (a) TS; (b) TSSA10; (c) TSSB10

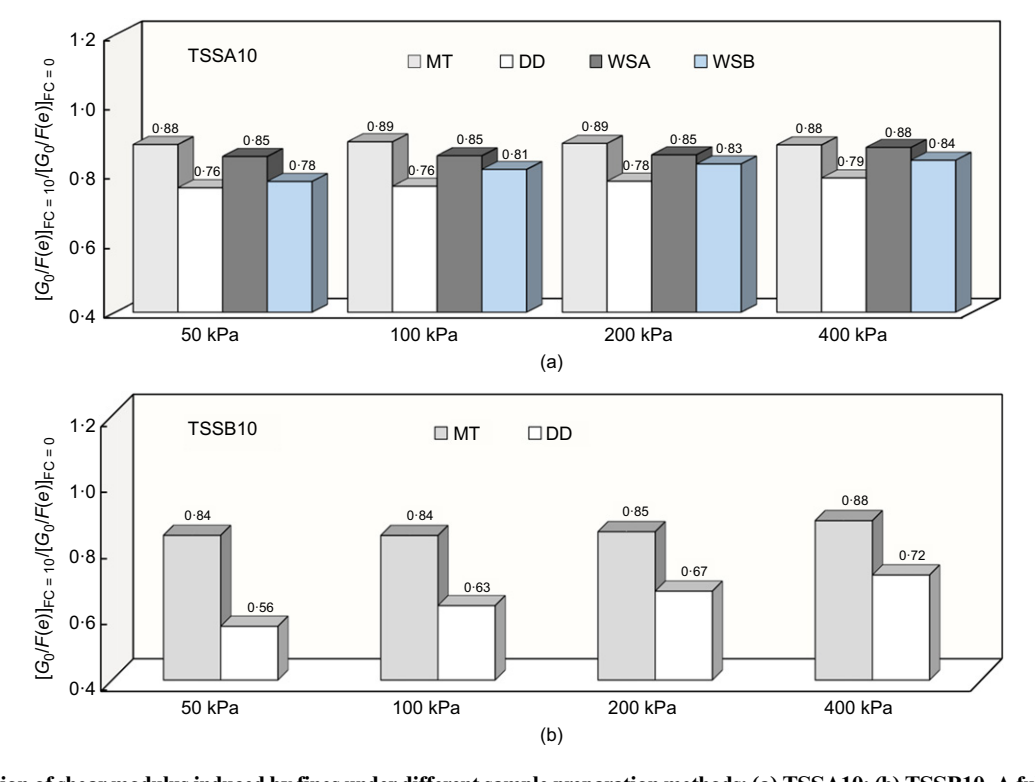


Fig. 12. Reduction of shear modulus induced by fines under different sample preparation methods: (a) TSSA10; (b) TSSB10. A full-colour version of this figure can be found on the ICE Virtual Library (www.icevirtuallibrary.com)

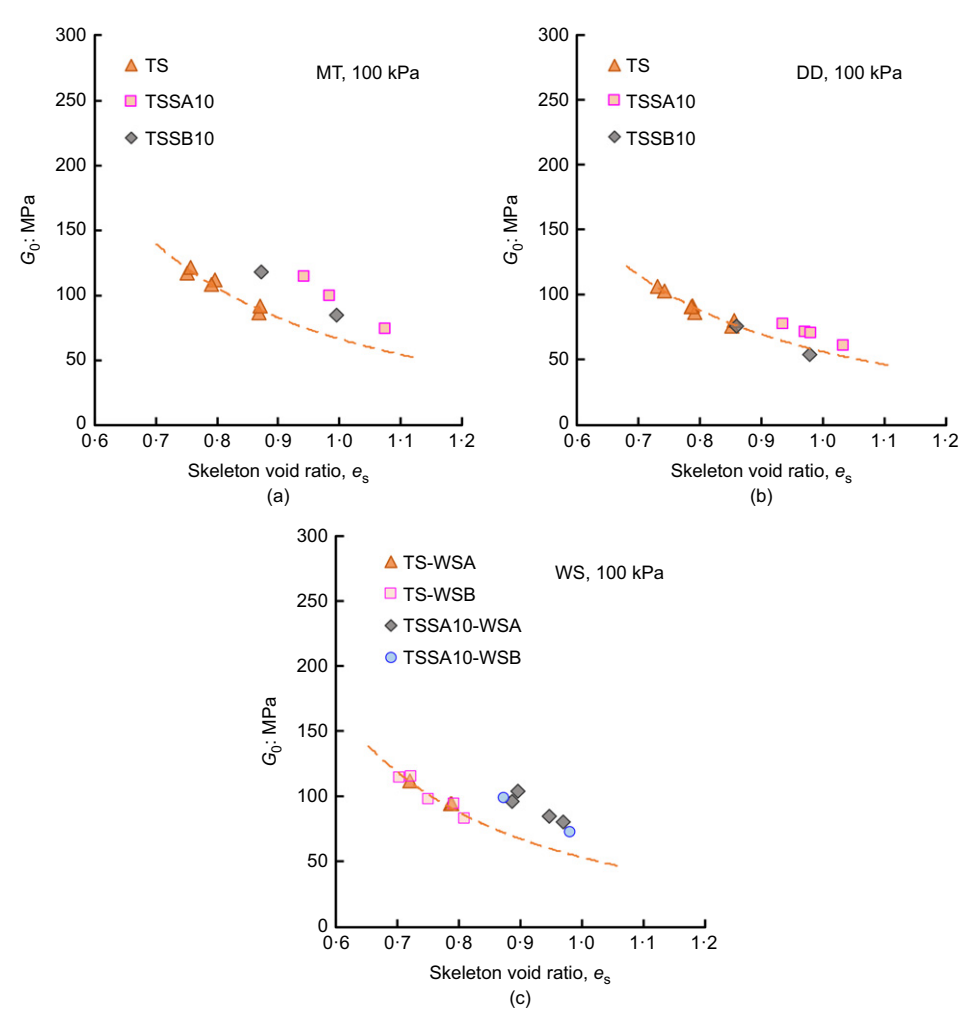


Fig. 13. Shear modulus plotted against skeleton void ratio: (a) MT specimens; (b) DD specimens; (c) WSA and WSB specimens

DD, WSA and WSB are notably lower than the calculated ones. It is worth noting that the difference tends to become larger for TSSA10 and TSSB10, especially for TSSB10. This implies that a combined influence of sample preparation and fines exists.

The results in Fig. 8 indicate that, either for TS, TSSA10 or TSSB10, the void ratio dependence of the specimens made by different methods seems to be similar and this dependence appears to be insensitive to the variation of confining stress. Note that the void ratio here is the post-consolidation void ratio corresponding to the given confining stress, not the initial void ratio prior to consolidation. To remove the influence of void ratio, the  $G_0$  value is divided by a widely used void ratio function (Kokusho, 1980; Yang & Liu, 2016)

$$F(e) = \frac{(2 \cdot 17 - e)^2}{1 + e} \tag{2}$$

The  $G_0/F(e)$  values plotted against void ratio for TS, TSSA10 and TSSB10 are shown in Fig. 10. For both clean and silty sands, the specimens made by MT always have the largest  $G_0/F(e)$  values, whereas the DD specimens have the lowest values. For clean sand, no notable differences are observed between WSA, WSB and DD specimens. However, when 10% of fines A are added, the  $G_0/F(e)$  values of WSA and WSB specimens become a little larger than that of DD specimens, especially at higher confining stress.

To better compare the influences of sample preparation on clean and silty sands, the average  $G_0/F(e)$  value of the specimens made by each of the three methods, DD, WSA

Table 3. Summary of b values for different mixtures prepared using different methods

Material-SPM	$\sigma'$	b value	Average b value
TSSA10-MT	50	0.75	0.75
	100	0.80	
	200	0.75	
	400	0.70	
TSSA10-DD	50	0.40	0.43
	100	0.40	
	200	0.45	
	400	0.45	
TSSA10-WSA/WSB	50	0.60	0.63
	100	0.70	
	200	0.60	
	400	0.60	
TSSB10-MT	50	0.55	0.58
	100	0.55	
	200	0.55	
	400	0.65	
TSSB10-DD	50	0.00	0.06
	100	0.00	
	200	0.05	
	400	0.20	

Note:  $\sigma'$ , effective confining stress (kPa); SPM, sample preparation method.

and WSB, is normalised by that of the MT specimens, defined as  $[G_0/F(e)]/[G_0/F(e)]_{MT}$ . This ratio can be used to quantify the difference in  $G_0$  value induced by different

sample preparation methods. In Fig. 11, the ratio is plotted against confining stress for TS, TSSA10 and TSSB10. It is clear that, for TS, the ratios for DD, WSA and WSB specimens are all located in a narrow range between 0·850 and 0·900. When it comes to TSSA10, the ratios for DD, WSA and WSB specimens become smaller, especially for the DD specimens. The ratio for DD specimens of TSSB10 is further reduced, with a value lower than 0·6 at the confining stress of 50 kPa, meaning that the  $G_0/F(e)$  value of DD specimens is approximately 40% smaller than that of MT specimens. These results suggest that the influence of sample preparation for sand with fines can be much enlarged as compared with that for clean sands and therefore cannot be simply neglected. Moreover, such influence is coupled with the size disparity between base sand and fines.

The role of fines in different sample preparations

To further investigate the combined influence of fines and sample preparation methods, the degradation of  $G_0/F(e)$  caused by fines is examined for specimens prepared by different methods. Fig. 12 shows the degradation ratio of  $G_0/F(e)$  induced by adding 10% fines of type A and B to the base sand. It is clear that the decrease of  $G_0/F(e)$  caused by the presence of fines is highly dependent on the sample preparation methods. For TSSA10, the reduction of  $G_0/F(e)$  for DD specimens is the strongest, whereas the degradation for MT specimens is the smallest. A similar phenomenon can also

be observed on TSSB10; nevertheless, the degree of degradation for DD specimens is much enlarged. It is worth noting that there are diverse views in the literature on the degradation of  $G_0$  due to the presence of non-plastic fines (Choo & Burns, 2015; Liu & Yang, 2018). Based on the findings here, one may attribute these diverse views to a combination of the influence of size disparity of coarse and fine particles and the influence of sample preparation method. Misleading conclusions may result from overlooking the combined effects.

To describe the influence of fines content on the properties of sand–fines mixtures, the skeleton void ratio, as defined in equation (3), has often been adopted in recent studies (Choo & Burns, 2015; Wichtmann *et al.*, 2015)

$$e_{\rm s} = \frac{e + f_{\rm c}}{1 - f_{\rm c}} \tag{3}$$

where e is the global void ratio and  $f_c$  is the fines content in decimal. Yang & Liu (2016) showed that the use of the skeleton void ratio significantly underestimates  $G_0$  values of sand–fines mixtures, even at a low percentage of fines (FC = 5% and 10%), and that the discrepancy can become larger as the quantity of fines increases. Here, an interesting question arises: is the use of the skeleton void ratio to characterise the influence of fines on  $G_0$  influenced by sample preparation methods? To answer the question, the  $G_0$  value plotted against the skeleton void ratio for specimens made by different methods under the confining pressure of 100 kPa is shown in Fig. 13.

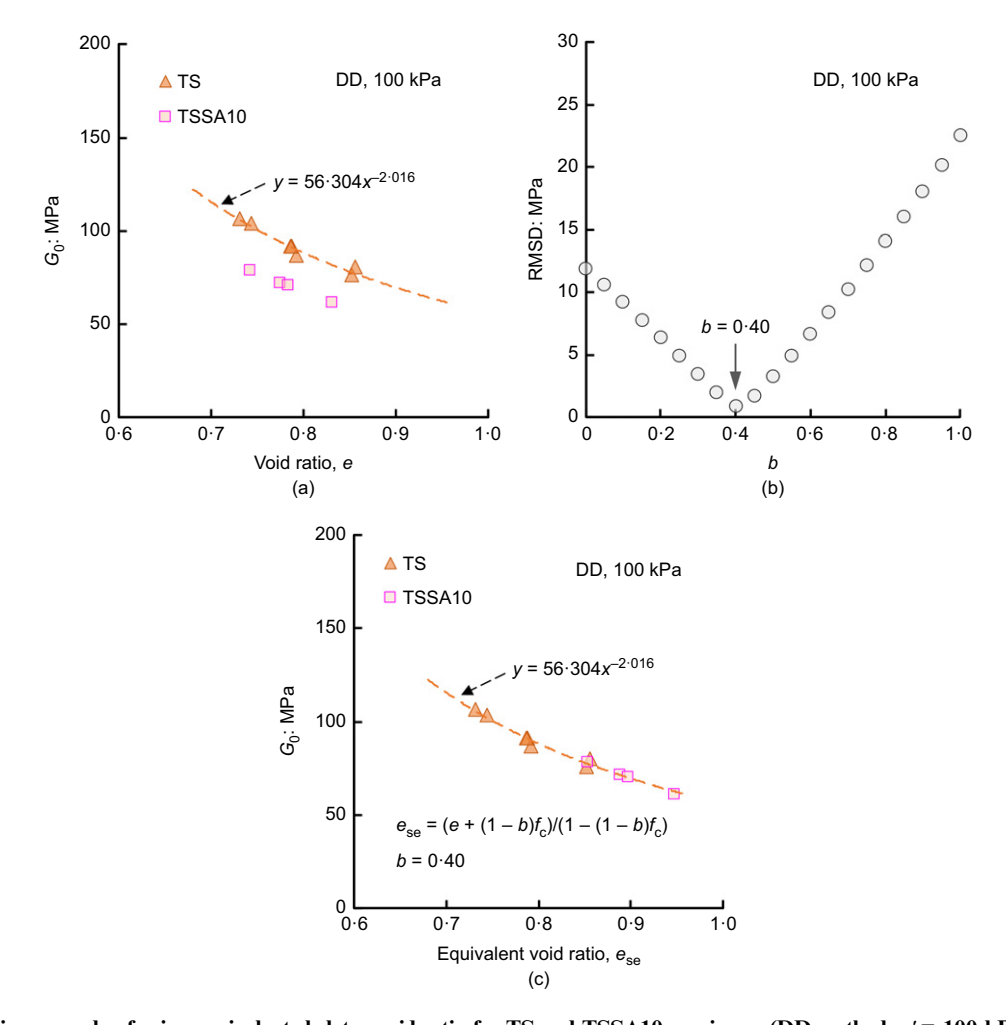


Fig. 14. Illustrative example of using equivalent skeleton void ratio for TS and TSSA10 specimens (DD method,  $\sigma' = 100$  kPa): (a)  $G_0$  plotted against global void ratio; (b) variations of RMSD with b; (c)  $G_0$  plotted against equivalent skeleton void ratio

For TSSA10, the data points of MT, WSA and WSB specimens obviously locate above the trend of TS, which means not all the fines play the role of voids. When the DD method is used, although the data points of TSSA10 are still above the trend of TS, the deviation is reduced compared with that of other sample preparation methods. For TSSB10, the data points of MT specimens are still located above the trend of TS, but the data points are almost in line with the trend of TS when the DD method is used. The implication is that the performance of the skeleton void ratio depends on the sample preparation method adopted and the size disparity of coarse and fine particles. An improved version of equation (3) is the so-called equivalent skeleton void ratio  $e_{\rm se}$ , as defined in equation (4), which assumes that part of the fines contribute to the force transfer (Thevanayagam et al., 2002; Rahman et al., 2008)

$$e_{\rm se} = \frac{e + (1 - b)f_{\rm c}}{1 - (1 - b)f_{\rm c}} \tag{4}$$

where factor b, varying between 0 and unity, is assumed to represent the fraction of fines that contribute to the force transfer. Obviously, when b is zero,  $e_{\rm se}$  equals  $e_{\rm s}$ , indicating that the fines act as voids; when b is unity,  $e_{\rm se}$  equals e, meaning that the fines act like the base sand.

To examine whether the equivalent skeleton void ratio works for the experimental data here, values of factor b are back-calculated using the procedure described in Yang

et al. (2015). The results are summarised in Table 3 for different sample preparation methods and an illustrative example is given in Fig. 14. It is interesting to note that, for a given mixture, the b value is highly dependent on the sample preparation method and the MT specimen generally has a much larger b value than the DD specimen. According to the assumed physical meaning of b, a larger b value indicates a larger fraction of fines participating in the force transfer. However, this does not seem to be consistent with the observed microstructures of the MT and DD specimens (Fig. 16). This inconsistency indicates that the b value does not always bear the assumed physical meaning, and it is not surprising given that the intergranular contacts of mixtures are highly complex, as noted by Carrera et al. (2011), Yang et al. (2015, 2018). Particle-level simulations of sand-fines mixtures have also found that the empirically determined b value is not consistent with the fraction of fines contributing to the force transfer (Luo & Yang, 2013).

#### Microscale considerations

Based on the discrete-element method (DEM), it has been found that at an approximately constant void ratio, the  $G_0$  of a granular packing increases as the coordination number and the uniformity of contact normal force distribution increase (Gu & Yang, 2013; Gu *et al.*, 2017). When fines are added to

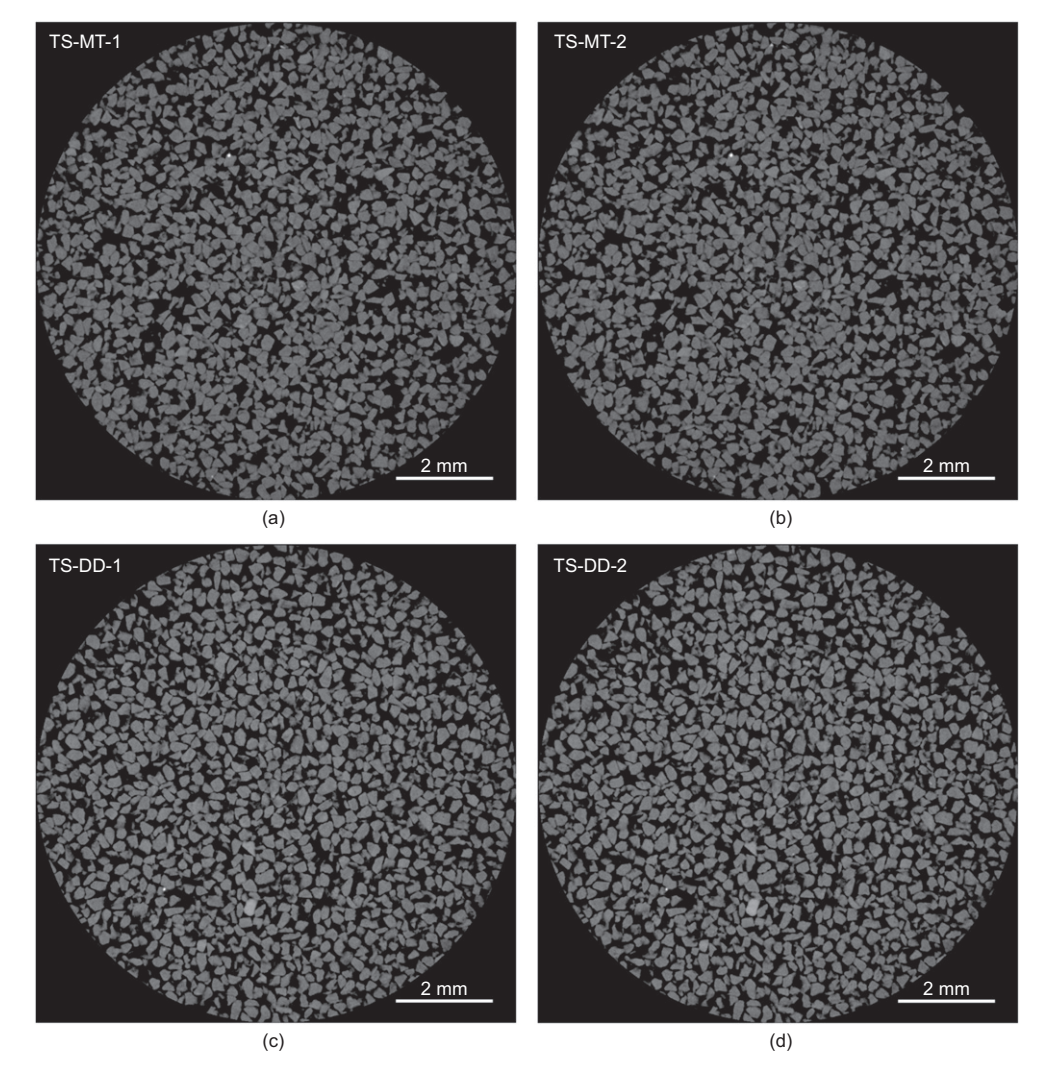


Fig. 15. X-ray images of TS specimens made by MT and DD methods: (a), (b) MT specimen; (c), (d) DD specimen

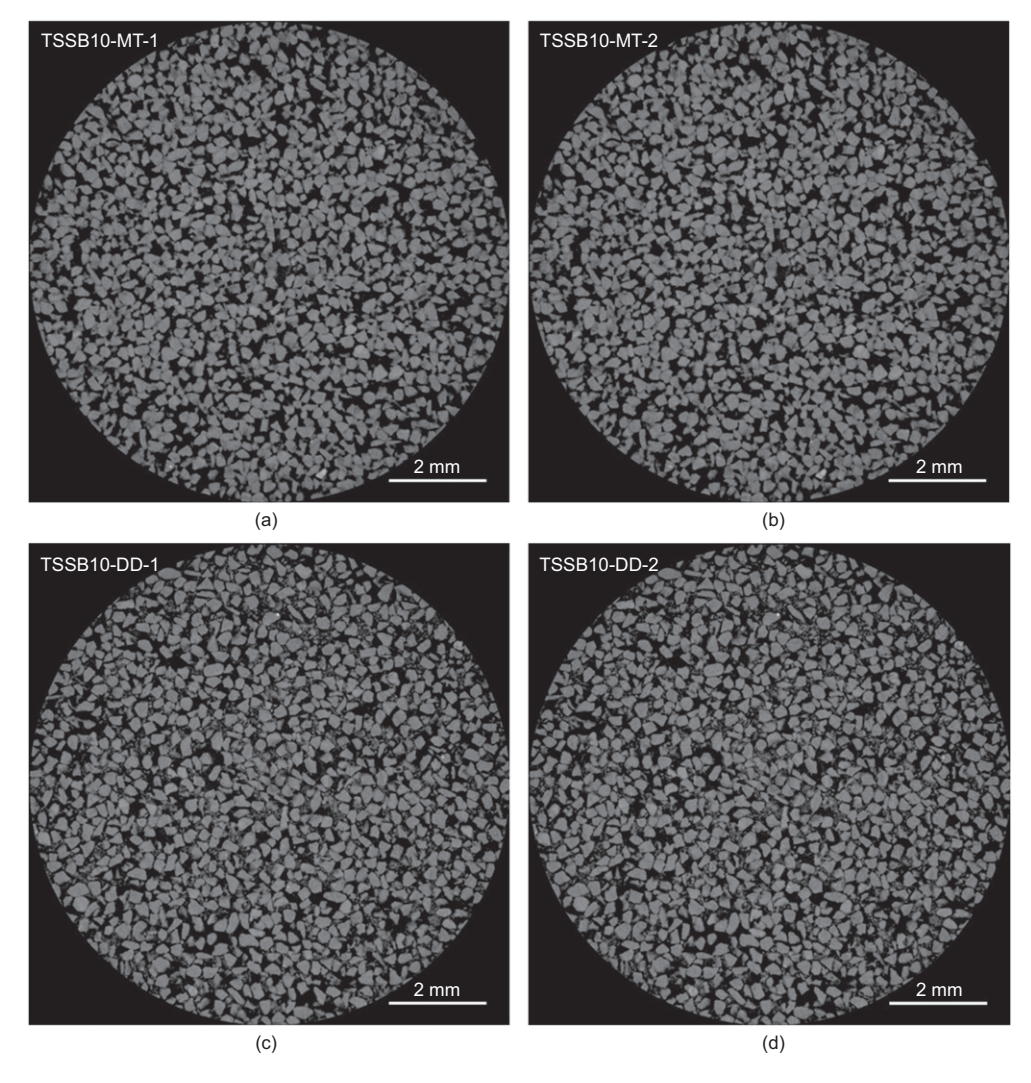


Fig. 16. X-ray images of TSSB10 specimens made by MT and DD methods: (a), (b) MT specimen; (c), (d) DD specimen

a base sand, the decrease of  $G_0$  at a constant void ratio is related to the decrease in coordination number (Yang & Liu, 2016; Gong *et al.*, 2019). However, the results in this study indicate that even if the same percentage of fines is added to the base sand, the reduction of  $G_0$  can be significantly influenced by the sample preparation method adopted. This phenomenon has not yet been reported in the literature; 'What is the underlying mechanism?' is an interesting question.

To address this question, the microstructures of TS and TSSB10 specimens, prepared by the MT method, are compared with those made by the DD method with the aid of the X-ray tomography technique, as shown in Figs 15 and 16. All the specimens were prepared at a similar global void ratio ( $\sim 0.750$ ) and all the images were obtained for horizontal sections. For TS, there is no observable difference between the microstructures of MT and DD specimens (Fig. 15). Note that the two images in Figs 15(a) and 15(b) represent two consecutive sections of the MT specimen and the other two images in Figs 15(c) and 15(d) are for two consecutive sections of the DD specimen. For TSSB10, however, the microstructures of MT and DD specimens appear to be different (Fig. 16): many small (fine) particles exist between large (sand) particles in the DD specimen, but no such observation is obtained on the MT specimen. Also, the distribution of the fine particles in the DD specimen appears to be non-uniform, with some fine particles clustering together between large sand grains. By comparison, the existence of fines in the MT specimen is not as clear as that in the DD specimen and the sand grains appear to have direct contacts with each other. When carefully comparing the microstructures of TS and TSSB10 specimens made by MT, it can be found that the outlines of sand grains in the TSSB10 specimen become blurred. This suggests that in the MT specimen, more fines are stuck on the surfaces of sand grains and the dominant contacts are those between large sand grains.

Based on the microscale observations, Fig. 17 presents four hypothesised microstructures: the case in Fig. 17(a) is for silty sand made by MT with a low size ratio; the case in Fig. 17(b) is for silty sand made by DD with a low size ratio; the case in Fig. 17(c) is for silty sand made by MT with a higher size ratio; and the case in Fig. 17(d) is for silty sand made by DD with a higher size ratio. All the four packings are assumed to have the same fines content and the same global void ratio, but the distributions and roles of fine particles are different. In the case shown in Fig. 17(a), more fines are stuck on the surfaces of the sand grains and the dominant contacts are those between sand grains. In the case in Fig. 17(b), more fines are involved in intergranular contacts in the form of sand-fine-sand contacts and sandfine-fine-sand contacts, thus forming a kind of metastable structure (Yamamuro et al., 2008; Dai et al., 2015; Yang et al., 2015). This is the possible reason why the DD specimens show lower values of shear stiffness and shear wave velocity than the MT specimens. When the size of fines

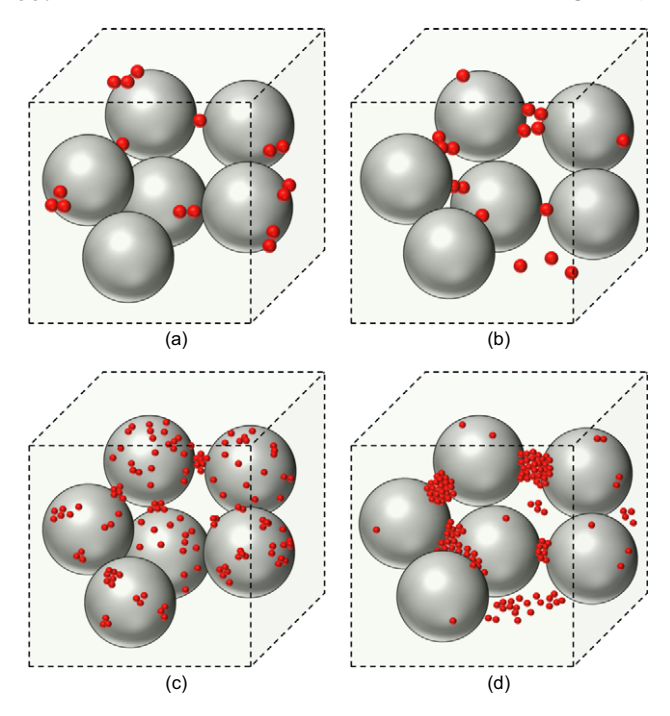


Fig. 17. Schematic illustration of intergranular contact conditions in silty sand with low fines content: (a) MT specimen with low size ratio; (b) DD specimen with low size ratio; (c) MT specimen with high size ratio; (d) DD specimen with high size ratio

becomes smaller (i.e. at higher size ratio), the number of metastable contacts (sand-fine-sand contacts and sand-fine-fine-sand contacts) increases significantly, particularly in the DD specimens, thus leading to more obvious reduction of shear stiffness and shear wave velocity. This explains the finding that the reduction of  $G_0$  with fines is much enlarged in the DD specimen than in the MT specimen when the size ratio became larger. Also, the packings in the cases shown in Figs 17(b) and 17(d) tend to give more severe non-uniformity in contact normal forces, thus leading to a further decrease in  $G_0$  value.

For WSA and WSB specimens, it is hypothesised that the intergranular contact conditions are between those of MT and DD specimens, thus leading to the experimental results that, under otherwise similar conditions, the  $G_0$  values of WSA and WSB specimens are larger than those of the DD specimens but smaller than those of the MT specimens. This finding is in agreement with the observation of Yamamuro *et al.* (2008) that the probability of occurrence of metastable contacts may be reduced in the water environment compared with the dry air environment.

The above microscale hypotheses are also supported by the isotropic compression behaviour of the specimens prepared by different methods, as shown in Fig. 18. To better demonstrate the difference induced by different sample preparation methods, the variation of volumetric strain during the isotropic compression is also determined. It is interesting to note that for TS specimens, different sample preparation methods do not induce significantly different volumetric strains (Fig. 18(b)), whereas

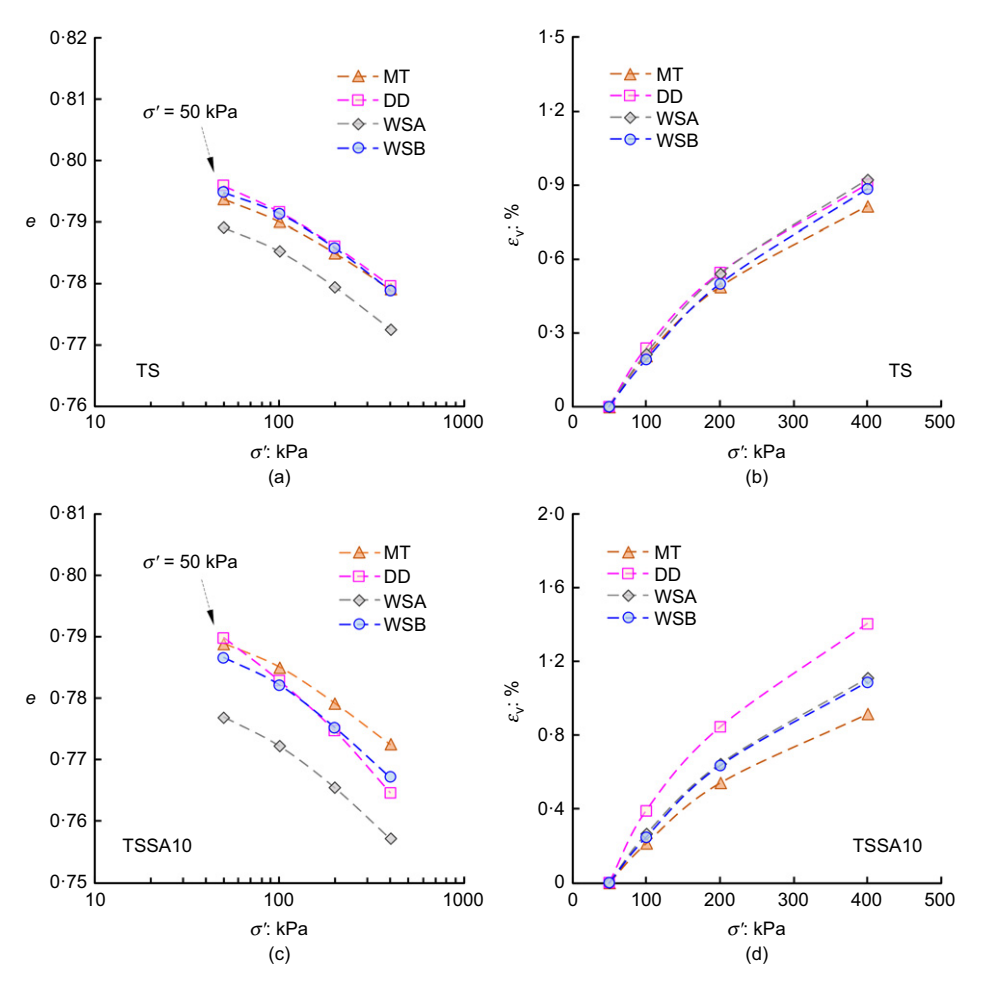


Fig. 18. Isotropic compression behaviour of TS and TSSA10 specimens made by different methods: (a, b) TS; (c, d) TSSA10

for TSSA10 specimens, different sample preparation methods can induce marked differences (Fig. 18(d)) and, in particular, the specimen formed by the DD method undergoes much larger volume changes compared with the specimen formed by the MT method. This finding is consistent with the hypothesis that more metastable contacts are present in the DD specimens.

# **CONCLUSIONS**

This paper presents first-hand experimental data showing how the sample reconstitution method affects the shear wave velocity or associated shear modulus of clean and silty sands. Four sample preparation methods, namely moist tamping (MT), dry deposition (DD), water sedimentation above and below water (WSA and WSB, respectively), have been systematically studied. The main findings resulting from the study are summarised as follows.

- (a) For clean Toyoura sand, the G<sub>0</sub> values of DD, WSA and WSB specimens are around 15% lower than that of the MT specimens, but there is no obvious difference in the G<sub>0</sub> values of DD, WSA and WSB specimens. For Toyoura sand mixed with 10% non-plastic fines, the difference in G<sub>0</sub> values of MT and DD specimens is greatly enlarged, especially for fines of smaller size, whereas the G<sub>0</sub> values of WSA and WSB specimens approximately locate between the G<sub>0</sub> values of MT and DD specimens.
- (b) The reduction of  $G_0$  with fines can be quite different when different sample preparation methods are used. For DD specimens, a marked reduction of  $G_0$  is observed compared with MT specimens, and the difference tends to become more significant when smaller fines are present. The performance of the skeleton void ratio or equivalent skeleton void ratio in accounting for the influence of fines is dependent on the adopted sample preparation method, and this dependence is a possible reason for the diverse performance of the two state variables in the literature.
- (c) A careful examination of the X-ray images suggests that the observed influence of sample preparation on  $G_0$  values of silty sand is mainly due to the difference in the microstructures formed. For MT specimens, more fines are stuck on the surfaces of sand grains and the sand–sand contacts are dominant, whereas for DD specimens, less stable contacts in the form of sand–fine–sand or sand–fine–fine–sand contacts tend to be dominant. This difference in intergranular contacts and thereafter in measured  $G_0$  values may become more significant when fines of smaller size are present.
- (d) The first-hand experimental data presented here can serve as a useful reference for validation of numerical and theoretical studies of the effect of fabric on small-strain stiffness of silty sands and contribute to a better understanding of the complex mechanical behaviour of granular materials.

# DATA AVAILABILITY STATEMENT

All data are available from the corresponding author upon reasonable request.

# ACKNOWLEDGEMENT

This work was supported by the Research Grants Council of Hong Kong (no. 17206119; C7038-20G). This support is gratefully acknowledged.

# **NOTATION**

- $b, f_{\rm c}$  parameters in equation (3)
- e,  $e_s$ ,  $e_{se}$  global void ratio, skeleton void ratio, equivalent
  - skeleton void ratio F(e) void ratio function
  - $G_0$  small-strain shear modulus
- $G_0/F(e)$  void ratio-corrected shear modulus
  - $G_{\rm s}$  specific gravity
  - V<sub>s</sub> shear wave velocity
  - $\varepsilon_{\rm v}$  volumetric strain
  - $\rho$  mass density involved in shear wave propagation
  - $\sigma'$  effective confining stress

# **REFERENCES**

- Alvarado, G. & Coop, M. C. (2012). On the performance of bender elements in triaxial tests. *Geotechnique* **62**, No. 1, 1–17, https://doi.org/10.1680/geot.7.00086.
- Carrera, A., Coop, M. & Lancellotta, R. (2011). Influence of grading on the mechanical behaviour of Stava tailings. *Géotechnique* 61, No. 11, 935–946, https://doi.org/10. 1680/geot.9.P.009.
- Chien, L. K. & Oh, Y. N. (2002). Influence of fines content and initial shear stress on dynamic properties of hydraulic reclaimed soil. *Can. Geotech. J.* 39, No. 1, 242–253, https://doi.org/10. 1139/t01-082.
- Choo, H. & Burns, S. E. (2014). Effect of over-consolidation ratio on dynamic properties of binary mixtures of silica particles. *Soil Dyn. Earthq. Engng* 60, 44–50, https://doi.org/10.1016/j.soildyn. 2014.01.015.
- Choo, H. & Burns, S. E. (2015). Shear wave velocity of granular mixtures of silica particles as a function of finer fraction, size ratios and void ratios. *Granular Matter* 17, No. 5, 567–578, https://doi.org/10.1007/s10035-015-0580-2.
- Clayton, C. R. I. (2011). Stiffness at small strain: research and practice. *Géotechnique* **61**, No. 1, 5–37, https://doi.org/10.1680/geot.2011.61.1.5.
- Dai, B., Yang, J. & Luo, X. (2015). A numerical analysis of the shear behavior of granular soil with fines. *Particuology* **21**, 160–172, https://doi.org/10.1016/j.partic.2014.08.010.
- Gong, J., Wang, X., Li, L. & Nie, Z. (2019). DEM study of the effect of fines content on the small-strain stiffness of gap-graded soils. *Comput. Geotech.* **112**, 35–40, https://doi.org/10.1016/j.compgeo. 2019.04.008
- Goudarzy, M., Rahman, M. M., König, D. & Schanz, T. (2016). Influence of non-plastic fines content on maximum shear modulus of granular materials. *Soils Found.* **56**, No. 6, 973–983, https://doi.org/10.1016/j.sandf.2016.11.003.
- Gu, X. Q. & Yang, J. (2013). A discrete element analysis of elastic properties of granular materials. *Granular Matter* **15**, No. 2, 139–147, https://doi.org/10.1007/s10035-013-0390-3.
- Gu, X. Q., Yang, J., Huang, M. S. & Gao, G. Y. (2015). Bender element tests in dry and saturated sand: signal interpretation and result comparison. *Soils Found.* 55, No. 5, 951–962, https://doi.org/10.1016/j.sandf.2015.09.002.
- Gu, X. Q., Lu, L. T. & Qian, J. G. (2017). Discrete element modeling of the effect of particle size distribution on the small strain stiffness of granular soils. *Particuology* **32**, 21–29, https://doi.org/10.1016/j.partic.2016.08.002.
- Hardin, B. O. & Richart, F. E. Jr. (1963). Elastic wave velocities in granular soils. *J. Soil Mech. Found. Div.* **89**, No. 1, 33–65, https://doi.org/10.1061/JSFEAQ.0000493.
- Ishihara, K. (1993). Liquefaction and flow failure during earth-quakes. *Géotechnique* 43, No. 3, 351–451, https://doi.org/10.1680/geot.1993.43.3.351.
- Iwasaki, T. & Tatsuoka, F. (1977). Effects of grain size and grading on dynamic shear moduli of sands. *Soils Found.* 17, No. 3, 19–35, https://doi.org/10.3208/sandf1972.17.3\_19.
- Kokusho, T. (1980). Cyclic triaxial test of dynamic soil properties for wide strain range. *Soils Found.* **20**, No. 2, 45–60, https://doi.org/10.3208/sandf1972.20.2\_45.
- Lade, P. V. & Yamamuro, J. A. (1997). Effects of nonplastic fines on static liquefaction of sands. *Can. Geotech. J.* 34, No. 6, 918–928, https://doi.org/10.1139/t97-052.

- Liu, X. & Yang, J. (2018). Influence of size disparity on small-strain shear modulus of sand-fines mixtures. *Soil Dyn. Earthq. Engng* 115, 217–224, https://doi.org/10.1016/j.soildyn. 2018.08.011.
- Luo, X. D. & Yang, J. (2013). Effects of fines on shear behavior of sand: a DEM analysis. In *Proceedings of the 5th international young* geotechnical engineers' conference (eds Y. J. Cui, F. Emeriault, F. Cuira, S. Ghabezloo, J. M. Pereira, M. Reboul, H. Ravel and A. M. Tang), pp. 265–268. Amsterdam, the Netherlands: IOS Press.
- Mulilis, J. P., Seed, H. B., Chan, C. K., Mitchell, J. K. & Arulanandan, K. (1977). Effects of sample preparation on sand liquefaction. J. Geotech. Engng Div. 103, No. 2, 91–108, https://doi.org/10.1061/ajgeb6.0000387.
- Payan, M., Senetakis, K., Khoshghalb, A. & Khalili, N. (2017). Characterization of the small-strain dynamic behaviour of silty sands; contribution of silica non-plastic fines content. *Soil Dyn. Earthq. Engng* 102, 232–240, https://doi.org/10.1016/j.soildyn. 2017.08.008.
- Rahman, M. M., Lo, S. R. & Gnanendran, C. T. (2008). On equivalent granular void ratio and steady state behaviour of loose sand with fines. *Can. Geotech. J.* 45, No. 10, 1439–1456, https://doi.org/eproxy.lib.hku.hk/10.1139/T08-064.
- Rahman, M. M., Cubrinovski, M. & Lo, S. R. (2012). Initial shear modulus of sandy soils and equivalent granular void ratio. *Geomech. Geoeng.* 7, No. 3, 219–226, https://doi.org/10.1080/ 17486025.2011.616935.
- Sahaphol, T. & Miura, S. (2005). Shear moduli of volcanic soils. *Soil Dyn. Earthq. Engng* **25**, No. 2, 157–165, https://doi.org/10.1016/j.soildyn.2004.10.001.
- Salgado, R., Bandini, P. & Karim, A. (2000). Shear strength and stiffness of silty sand. J. Geotech. Geoenviron. Engng 126, No. 5, 451–462, https://doi.org/10.1061/(asce)1090-0241(2000)126:5 (451).
- Shi, J. Q., Haegeman, W. & Xu, T. (2020). Effect of non-plastic fines on the anisotropic small strain stiffness of a calcareous sand. *Soil Dyn. Earthq. Eng.* 13, 106381, https://doi.org/10.1016/j.soildyn. 2020.106381.
- Shi, J. Q., Haegeman, W. & Cnudde, V. (2021). Anisotropic small-strain stiffness of calcareous sand affected by sample preparation, particle characteristic and gradation. *Géotechnique* 71, No. 4, 305–319, https://doi.org/10.1680/jgeot.18.P.348.
- Stokoe, K. H., Darendeli, M. B., Andrus, R. D. & Brown, L. T. (1999). Dynamic soil properties: laboratory, field and correlation studies. In *Proceedings of the 2nd international conference on earthquake geotechnical engineering* (ed. P. Seco e Pinto), vol. 3, pp. 811–845. Rotterdam, the Netherlands: A. A. Balkema.
- Sze, H. Y. & Yang, J. (2014). Failure modes of sand in undrained cyclic loading: impact of sample preparation. *J. Geotech. Geoenviron. Engng* 140, No. 1, 152–169, https://doi.org/10. 1061/(ASCE)GT.1943-5606.0000971.
- Thevanayagam, S., Shenthan, T., Mohan, S. & Liang, J. (2002). Undrained fragility of clean sands, silty sands, and sandy silts.

- *J. Geotech. Geoenviron. Engng* **128**, No. 10, 849–859, https://doi.org/10.1061/(asce)1090-0241(2002)128:10(849).
- Wichtmann, T., Navarrete Hernández, M. A. & Triantafyllidis, T. (2015). On the influence of a non-cohesive fines content on small strain stiffness, modulus degradation and damping of quartz sand. *Soil Dyn. Earthq. Engng* **69**, 103–114, https://doi.org/10.1016/j.soildyn.2014.10.017.
- Wichtmann, T., Steller, K. & Triantafyllidis, T. (2020). On the influence of the sample preparation method on strain accumulation in sand under high-cyclic loading. Soil Dyn. Earthq. Engng 131, 106028, https://doi.org/10.1016/j.soildyn.2019. 106028.
- Wood, F. M., Yamamuro, J. A. & Lade, P. V. (2008). Effect of depositional method on the undrained response of silty sand. *Can. Geotech. J.* 45, No. 11, 1525–1537, https://doi.org/10. 1139/T08-079.
- Yamamuro, J. A., Wood, F. M. & Lade, P. V. (2008). Effect of depositional method on the microstructure of silty sand. *Can. Geotech. J.* 45, No. 11, 1538–1555, https://doi.org/10. 1139/T08-080.
- Yamashita, S., Kawaguchi, T., Nakata, Y., Mikamt, T., Fujiwara, T. & Shibuya, S. (2009). Interpretation of international parallel test on the measurement of *G*<sub>max</sub> using bender elements. *Soils Found.* **49**, No. 4, 631–650, https://doi.org/10.3208/sandf.49.631.
- Yang, J. & Gu, X. Q. (2013). Shear stiffness of granular material at small strains: does it depend on grain size? *Géotechnique* 63, No. 2, 165–179, https://doi.org/10.1680/geot.11.P.083.
- Yang, J. & Liu, X. (2016). Shear wave velocity and stiffness of sand: the role of non-plastic fines. *Géotechnique* 66, No. 6, 500–514, https://doi.org/10.1680/jgeot.15.P.205.
- Yang, J. & Wei, L. M. (2012). Collapse of loose sand with the addition of fines: the role of particle shape. *Géotechnique* 62, No. 12, 1111–1125, https://doi.org/10.1680/geot.11.P.062.
- Yang, Z. X., Li, X. S. & Yang, J. (2008). Quantifying and modelling fabric anisotropy of granular soils. *Géotechnique* 58, No. 4, 237–248, https://doi.org/10.1680/geot.2008.58.4.237.
- Yang, J., Wei, L. M. & Dai, B. B. (2015). State variables for silty sands: global void ratio or skeleton void ratio? *Soils Found.* 55, No. 1, 99–111, https://doi.org/10.1016/j.sandf.2014.12.008.
- Yang, J., Liu, X., Rahman, M. M., Lo, R., Goudarzy, M. & Schanz, T. (2018). Shear wave velocity and stiffness of sand: the role of non-plastic fines. *Géotechnique* 68, No. 10, 931–934, https://doi.org/10.1680/jgeot.16.D.006.
- Youn, J. U., Choo, Y. W. & Kim, D. S. (2008). Measurement of small-strain shear modulus G<sub>max</sub> of dry and saturated sands by bender element, resonant column, and torsional shear tests. *Can. Geotech. J.* 45, No. 10, 1426–1438, https://doi.org/10. 1139/T08-069.
- Zhu, Z. H., Zhang, F., Dupla, J. C., Canou, J., Foerster, E. & Peng, Q. Y. (2021). Assessment of tamping-based specimen preparation methods on static liquefaction of loose silty sand. *Soil Dyn. Earthq. Engng* 143, 106592, https://doi.org/10.1016/j. soildyn.2021.106592.